International Journal of Science, Environment
and Technology, Vol. 2, No 1, 2013, 60 - 79

A TWO DIMENSIONAL NUMERICAL MODEL OF PRIMARY POLLUTANT EMITTED FROM AN URBAN AREA SOURCE WITH WET DEPOSITION AND MESOSCALE WIND

Lakshminarayanachari K[1], CM Suresha[2*], M Siddalinga Prasad[3] & Pandurangappa C[4]
[1]Department of Mathematics, Sai Vidya Institute of Technology, Rajanukunte,
Bangalore - 560 064, INDIA
[2]Department of Mathematics, R N S Institute of Technology, Channasandra,
Bangalore-560 098, INDIA
[3]Department of Mathematics, Siddaganga Institute of Technology, Tumkur-572103, INDIA.
[4]Department of Mathematics, Raja Rajeswari College of Engineering,
Bangalore-560 074, INDIA.
Emails: [1]lncspcms@gmail.com, [2]msuresha2006@gmail.com, [3]msp_maths@rediffmail.com,
[4]pandurangappa_c@yahoo.co.in (**Corresponding Author*)

Abstract: A Numerical Model has been developed to study the dispersion of primary pollutant emitted from an urban area source considering the large scale and mesoscale winds. The model takes into account the removal mechanisms such as wet deposition, dry deposition and gravitational settling processes. The obtained numerical model is based on solving the equations by using implicit Crank-Nicolson finite difference scheme under stability dependent meteorological parameters involved in wind velocities and eddy diffusivity profiles. The mesoscale wind is chosen to simulate the local wind produced by urban heat island. The results show that the effect of the mesoscale wind on primary pollutants is a decrease in the concentration in the upwind side of the center of heat island and an increase in the concentration in the downwind side of the center of heat island.
Keywords: Air pollution model, Mesoscale wind, Primary pollutant, Chemical reaction, Crank-Nicolson implicit method, Deposition velocity.

1. INTRODUCTION

The dispersion of atmospheric contaminant has become a global problem in the recent years due to rapid industrialization and urbanization. The toxic gases and small particles could accumulate in large quantities over urban areas, under certain meteorological conditions. This is one of the serious health hazards in many of the cities in the world. An acute exposure to the elevated levels of particulate air pollution has been associated with the cases of increased cardiopulmonary mortality, hospitalization for respiratory diseases, exacerbation of asthma, decline in lung function, and restricted life activity. Small deficits in lung function, higher risk of chronic respiratory disease and increased mortality have also been associated with chronic exposure to respirable particulate air pollution [1].

*Received Dec 26, 2012 * Published Feb 2, 2013 * www.ijset.net*

Epidemiological studies have demonstrated a consistent increased risk for cardiovascular functions in relation to both short- and long-term exposure to the present-day concentrations of ambient particulate matter [2]. Exposure to the fine airborne particulate matter is associated with cardiovascular functions and mortality in older and cardiac patients [3]. Volatile organic compounds (VOCs), which are molecules typically containing 1–18 carbon atoms that readily volatilize from the solid or liquid state, are considered a major source of indoor air pollution and have been associated with various adverse health effects including infection and irritation of respiratory tract, irritation to eyes, allergic skin reaction, bronchitis, and dyspnea [4, 5, 6].

There are some earlier studies in which measurements (usually airborne) of dispersion of air pollutants carried out in urban complexes in order to obtain material balances on gaseous and particulate pollutants [7, 8]. Acid precipitation can occur when particles and gases are removed from the atmosphere by (i) rain and snow (wet deposition) (ii) by impaction on water, soil and vegetation surfaces (dry deposition) and (iii) gravitational settling velocity. The transformation of gases to particles in the atmosphere and the deposition rates of gases and particles are a function of meteorological conditions over a time as well as the distribution of emission sources. In order to justify checks on emissions of acid precursors, the relationship between a source and the deposition pattern that it produces needs to be understood. This is difficult to accomplish by field monitoring. Mathematical models are the only way to estimate the relative contribution of sources to the total deposition at a particular receptor over a long period of time. In this context the study of air pollution using numerical methods is highly important.

The numerical area-source model [9] considers eddy diffusivity and velocity profiles as functions of vertical height (z), stability parameter and frictional velocity. In this model the geostrophic wind, net heat fluxes, surface roughness, mixing height of the atmosphere and emission rate of the source are specified. Mass conservation equations for an array of boxes (or nodes) are solved simultaneously by an implicit finite difference scheme for different atmospheric conditions. The pollutant concentration is determined for the steady state and without the removal mechanisms. The numerical model [10] is a time dependent and two-dimensional model. This model deals with chemically inactive primary pollutant and also it does not take into account the transformation and removal processes. Shir and Shieh [11] developed a generalized urban air pollution model and applied it to the study of diffusion of sulphur dioxide in the St. Louis metropolitan area.

Davidson [12] and Chandler [13] commented that near the center of heat island the vertical mixing would be enhanced by mesoscale wind. There are numerous models [14, 15, 16] to deal with the dispersion of pollutants emitted from point source, line source and area source. In these models eddy-diffusivity and velocity profiles are all considered constant. [17, 18, 19, 20, 21, 22, 23] have studied mathematical models with chemically reactive pollutants. However these models do not take into account the mesoscale wind. The present study takes into account the effect of mesoscale wind and the distribution of pollutants in the atmosphere over the urban areas.

One of the important aspects of mathematical modeling of air pollution which requires immediate attention is the study of the diffusion of air pollutants in an urban area. Large urban areas generate local or mesoscale wind, due to urban heat island. In this paper we develop a numerical model for primary pollutant in the atmosphere with more realistic large scale and mesoscale wind velocities and eddy diffusivity profiles. We study the effect of removal mechanisms such as dry deposition, wet deposition and gravitational settling velocity on primary pollutants.

2. Model development

The physical problem consists of an area source, which is spread over the surface of a city with finite downwind distance and infinite cross wind dimensions. We assume that the pollutants are emitted at a constant rate from the area source and spread within the mixing layer adjacent to earth's surface where mixing takes place as a result of turbulence and convective motion. This mixing layer extends upwards from the surface to a height where all turbulent flux-divergences resulting from surface action have virtually fallen to zero. The pollutants are transported horizontally by large scale wind which is a function of vertical height (z) and horizontally as well as vertically by the local mesoscale wind. We have considered the centre of the heat island at a distance $x = l/2$ i.e. at the centre of the city. We have considered the source region within the urban area which extends to a distance l in the downwind x direction ($0 \le x \le l$). In this model we have taken l = 6 km. Assuming the homogeneity of urban terrain, the mean concentration of pollutant is considered to be the constant along the crosswind direction i.e., pollutants concentration does not vary in cross wind direction. Therefore, there is no y-dependence. Also lateral flux of pollutants is small and it traverses the centre line of uniform area source. The physical description of the model is shown schematically in Figure 1 we intend to compute the concentration distribution of the

primary pollutant in the urban area. We assume that the pollutants undergo the removal mechanisms, such as dry deposition, wet deposition and gravitational settling

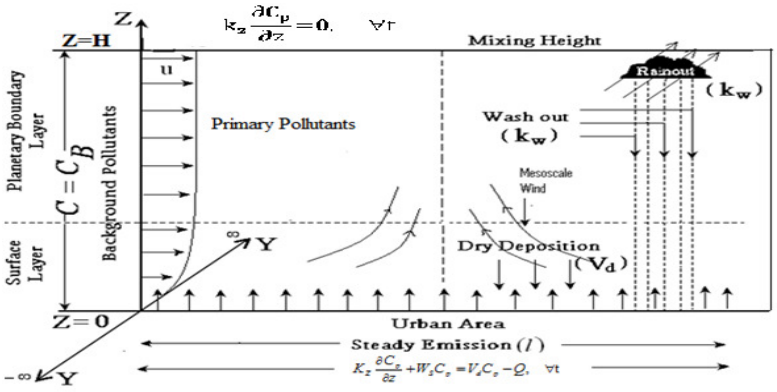

Fig 1: Physical layout of the model

2.1 Primary pollutant

The basic governing equation of primary pollutant can be written as

$$\frac{\partial C_p}{\partial t} + U(x,z)\frac{\partial C_p}{\partial x} + W(z)\frac{\partial C_p}{\partial z} = \frac{\partial}{\partial z}\left(K_z(z)\frac{\partial C_p}{\partial z}\right) - k_{wp}C_p \tag{1}$$

where $C_p = C_p(x,z,t)$ is the ambient mean concentration of pollutant species, U is the mean wind speed in x-direction, W is the mean wind speed in z-direction, K_z is the turbulent eddy diffusivity in z-direction, k_{wp} is the first order rainout/washout coefficient of primary pollutant C_p. Eq. (1) is derived under the following assumptions:

1. The lateral flux of pollutants along crosswind direction is assumed to be small i.e., $V\frac{\partial C_p}{\partial y}$ and $\frac{\partial}{\partial y}\left(K_y\frac{\partial C_p}{\partial y}\right) \to 0$, where V is the velocity in the y direction and K_y is the eddy-diffusivity coefficient in the y direction.
2. Horizontal advection is greater than horizontal diffusion for not too small values of wind velocity, i.e., meteorological conditions are far from stagnation. The horizontal advection by the wind dominates over horizontal diffusion, i.e., $U\frac{\partial C_p}{\partial x} \gg \frac{\partial}{\partial x}\left(K_x\frac{\partial C_p}{\partial x}\right)$, where U and K_x are the horizontal wind velocity and horizontal eddy diffusivity along x direction respectively.

We assume that the region of interest is free from pollution at the beginning of the emission. Thus, the initial condition is

$$C_p = 0 \quad at \quad t = 0,\ 0 \le x \le l \quad and \quad 0 \le z \le H \tag{2}$$

where l is the length of desired domain of interest in the wind direction and H is the mixing

height. We assume that there is no background pollution of concentration entering at $x = 0$ into the domain of interest. Thus

$$C_p = 0 \quad at \quad x = 0,\ 0 \le z \le H \quad and \quad \forall\ t > 0 \tag{3}$$

We assume that the chemically reactive air pollutants are being emitted at a steady rate from the ground level. They are removed from the atmosphere by ground absorption and gravitational settling. Hence the corresponding boundary condition takes the form

$$K_z \frac{\partial C_p}{\partial z} + W_s C_p = V_{dp} C_p - Q \ \ at \quad z = 0,\ 0 < x \le l \ and \ \forall \ t > 0 \tag{4}$$

where Q is the emission rate of primary pollutant species and V_{dp} is the dry deposition velocity and W_S is the gravitational settling of primary pollutants.

The pollutants are confined within the mixing height and there is no leakage across the top boundary of the mixing layer. Thus,

$$K_z \frac{\partial C_p}{\partial z} = 0 \quad at \quad z = H, \quad 0 < x \le l \ and \ \forall \ t > 0 \tag{5}$$

3. Meteorological parameters

The treatment of Eq. (1) mainly depends on the proper estimation of diffusivity coefficient and velocity profile of the wind near the ground/or the lower layers of the atmosphere. The meteorological parameters influencing eddy diffusivity and velocity profile are dependent on the intensity of turbulence, which is influenced by atmospheric stability. Stability near the ground is dependent primarily upon the net heat flux. In terms of boundary layer notation, the atmospheric stability is characterized by the parameter L [24], which is also a function of net heat flux among several other meteorological parameters. It is defined by

$$L = -\frac{u_*^3 \tilde{n} C_p T}{\hat{e} g H_f} \tag{6}$$

where u_* is the friction velocity, H_f the net heat flux, ρ the ambient air density, C_p the specific heat at constant pressure, T the ambient temperature near the surface, g the gravitational acceleration and $\hat{e}$ the Karman's constant ≈ 0.4. $H_f < 0$ and consequently $L > 0$ represents stable atmosphere, $H_f > 0$ and $L < 0$ represent unstable atmosphere and $H_f = 0$ and $L \to \infty$ represent neutral condition of the atmosphere.

The friction velocity u_* is defined in terms of geostrophic drag coefficient c_g and geostrophic wind u_g such that $u_* = c_g u_g$ (7)

where c_g is a function of the surface Rossby number $R_0 = u_*/fz_0$, where f is the Coriolis parameter due to earth's rotation and z_0 is the surface roughness length. [25] gave the value of c_{gn}, the drag coefficient for a neutral atmosphere in the form

$$c_{gn} = \frac{0.16}{\log_{10}(R_0) - 1.8} \tag{8}$$

The effect of thermal stratification on the drag coefficient can be accounted through the relations: $c_{gus} = 1.2\, c_{gn}$ for unstable flow, (9)

$c_{gs} = 0.8\, c_{gn}$ for slightly stable flow and (10)

$c_{gs} = 0.6\, c_{gn}$ for stable flow. (11)

In order to evaluate the drag coefficient, the surface roughness length z_0 may be computed according to the relationship developed by [25] i.e., $z_0 = (\bar{H}\, a)/(2\bar{A})$, where $\bar{H}$ is the effective height of roughness elements, a is the frontal area seen by the wind and $\bar{A}$ is the lot area (i.e., the total area of the region divided by the number of elements).

Finally, in order to connect the stability length L to the Pasquill stability categories, it is necessary to quantify the net radiation index. Ragland [9] used the following values of H_f (Table 1) for urban area.

Table 1: Net heat flux $H_f(langley\ min^{-1})$

Net radiating index	4.0	3.0	2.0	1.0	0.0	-1.0	-2.0
Net heat flux H_f	0.24	0.18	0.12	0.06	0.0	-0.03	-0.06

3.1 Eddy diffusivity profiles

The common characteristics of K_z is that it has linear variation near the ground, a constant value at mid mixing depth and a decreasing trend as the top of the mixing layer is approached. Shir [26] gave an expression based on theoretical analysis of neutral boundary layer in the form

$K_z = 0.4u_*ze^{-4z/H}$, where H is the mixing height. (12)

For stable condition, Ku et al. [27] used the following form of eddy-diffusivity,

$$K_z = \frac{\hat{e}u_*z}{0.74+4.7z/L} exp(-b\c{c}),\ b = 0.91,\ \c{c} = z/\left(L\sqrt{\grave{\imath}}\right),\quad \grave{\imath} = u_*/|fL| \tag{13}$$

The above form of K_z was derived from a higher order turbulence closure model which was tested with stable boundary layer data of Kansas and Minnesota experiments. Eddy-diffusivity profiles given by Eq. (11) and Eq. (12) have been used in this model for neutral and stable atmospheric conditions.

3.2 Wind Velocity Profiles

In order to incorporate realistic form of velocity profile which depends on Coriolis force, surface friction, geostrophic wind, stability characterizing parameter L and vertical height z, we integrate the velocity gradient from z_0 to $z + z_0$ for neutral and stable conditions. So we obtain the following expressions for wind velocity.

In case of neutral stability with $z < 0.1\kappa(u_* / f)$, we get $U = \frac{u_*}{\kappa}\ln\left(\frac{z+z_0}{z_0}\right)$ (14)

In case of stable flow with $0 < z/L < 1$, we get $U = \frac{u_*}{\kappa}\ln\frac{z+z_0}{z_0} + \frac{\alpha}{L}z$ (15)

In case of stable flow with $1 < z/L < 6$, we get $U = \frac{u_*}{\kappa}\ln\frac{z+z_0}{z_0} + 5.2$ (16)

In the planetary boundary layer, above the surface layer, power law scheme has been employed. $U = (u_g - u_{sl})\left(\frac{z-z_{sl}}{H-z_{sl}}\right)^p + u_{sl}$, (17)

where, u_g is the geostrophic wind, u_{sl} is the wind at z_{sl}, z_{sl} the top of the surface layer, H the mixing height and p is an exponent which depends upon the atmospheric stability. Jones et al. [28] suggested the values for the exponent p, obtained from the measurements made from urban wind profiles, as follows:

$$p = \begin{cases} 0.2 \text{ for neutral condition,} \\ 0.35 \text{ for slightly stable flow and,} \\ 0.5 \text{ for stable flow.} \end{cases}$$

Wind velocity profiles given by equations (14)-(17) due to Ragland [9] are used in our model.

3.3 Mesoscale wind velocity profiles

It is known that in an urban city the heat generation causes the vertical flow of air with maximum velocity (rising of air) at the centre of the city. Hence the city can be called heat island. This rising air forms an air circulation and this circulation is completed at larger heights. This is called mesoscale circulation. In order to incorporate more realistic form of velocity profile in the models Ragland [9], Kakamari [21] and Lakshminarayanachari [22], integrate equation $\frac{\partial U}{\partial z} = \frac{u_*\phi_M}{\hat{e}z}$ from $z_o \; to \; z + z_o$ for the stable and the neutral conditions which depend on Coriolis force, surface friction, geostrophic wind, stability characteristic parameter L and vertical height z. But large urban areas generate an additional Mesoscale circulation. The velocity profiles of the above models are not sufficient to predict the concentration distribution over the urban areas. Dilley-Yen [14] have considered the

mesoscale wind velocity profiles for simple power law profile of large scale wind. Therefore, to take into account the mesoscale wind over the urban areas, for realistic form of velocity profiles, it is necessary to modify the wind velocity profiles of Regland [9] as per Dilley-Yen [14]. So, we obtain the following expressions for large and mesoscale wind velocities.

In case of neutral stability with $z < 0.1\hat{e}\frac{u_*}{f}$, we get $U = \frac{u_*}{\hat{e}}\ln\left(\frac{z+z_0}{z_0}\right)$ (18)

It is assumed that the horizontal mesoscale wind varies in the same vertical manner as u. The vertical mesoscale wind W_e can then be found by integrating the continuity equation and we obtain in the form $U_e = -a(x - x_o)\ln\left(\frac{z+z_0}{z_0}\right)$ (19)

where *a* is proportionality constant. Thus we have

$$U(x,z) = u + u_e = \left(\frac{u_*}{\hat{e}} - a(x - x_o)\right)\ln\left(\frac{z+z_0}{z_0}\right) \quad (20)$$

$$W(z) = W_e = a\left[z\ln\left(\frac{z+z_0}{z_0}\right) - z + z_0 ln(z + z_0)\right] \quad (21)$$

In case of stable flow with $0 < z/L < 1$, we get $U = \frac{u_*}{\hat{e}}\left[\ln\left(\frac{z+z_0}{z_0}\right) + \frac{\acute{a}}{L}z\right]$ (22)

$$U_e = -a(x - x_o)\left[\ln\left(\frac{z+z_0}{z_0}\right) + \frac{\acute{a}}{L}z\right] \quad (23)$$

$$U(x,z) = u + u_e = \left(\frac{u_*}{\hat{e}} - a(x - x_o)\right)\left[\ln\left(\frac{z+z_0}{z_0}\right) + \frac{\acute{a}}{L}z\right] \quad (24)$$

$$W(z) = W_e = a\left[z\ln\left(\frac{z+z_0}{z_0}\right) - z + z_0 ln(z + z_0) + \frac{\acute{a}}{2L}z^2\right] \quad (25)$$

In case of stable flow with $1 < z/L < 6$, we get $U = \frac{u_*}{\hat{e}}\left[\ln\left(\frac{z+z_0}{z_0}\right) + 5.2\right]$ (26)

$$U_e = -a(x - x_o)\left[\ln\left(\frac{z+z_0}{z_0}\right) + 5.2\right] \quad (27)$$

$$U(x,z) = u + u_e = \left(\frac{u_*}{\hat{e}} - a(x - x_o)\right)\left[\ln\left(\frac{z+z_0}{z_0}\right) + 5.2\right] \quad (28)$$

$$W(z) = W_e = a\left[z\ln\left(\frac{z+z_0}{z_0}\right) + z_0 ln(z + z_0) + 4.2z\right] \quad (29)$$

In the planetary boundary layer, above the surface layer, power law scheme has been employed. $U = (u_g - u_{sl})\left(\frac{z-z_{sl}}{H-z_{sl}}\right)^p + u_{sl}$ (30)

$$U_e = -a(x - x_o)\left[\left(\frac{z-z_{sl}}{H-z_{sl}}\right)^p + u_{sl}\right] \quad (31)$$

$$U(x,z) = u + u_e = \left[(u_g - u_{sl}) - a(x - x_o)\right]\left[\left(\frac{z-z_{sl}}{H-z_{sl}}\right)^p + (1 - a(x - x_o))u_{sl}\right] \quad (32)$$

$$W(z) = W_e = a\left[\frac{(z-z_{sl})}{p+1}\left(\frac{z-z_{sl}}{H-z_{sl}}\right)^p + zu_{sl}\right] \quad (33)$$

where, u_g is the geostrophic wind, u_{sl} the wind at $z_{sl,}$ z_{sl} the top of the surface layer, x_0 is the x −co-ordinate of the centre of heat island, H the mixing height and p is an exponent which depends upon the atmospheric stability. Jones et al. [28] suggested values for the exponent p, obtained from the measurements made from urban wind profiles, as follows;

$$\mathrm{p} = \begin{cases} 0.20 & \text{for neutral condition} \\ 0.35 & \text{for slightly stable flow} \\ 0.50 & \text{for stable flow} \end{cases}$$

Wind velocity profiles given by equations (18), (22), (26) and (30) are due to Ragland [9] equations (24), (25), (28), (29), (32) and (33) are modified as per Dilley –Yen [14] are used in this model.

4. Numerical method

It is difficult to obtain the analytical solution for equation (1) because of the complicated form of wind speed and eddy diffusivity profiles considered in this model. Hence, we have used numerical method based on Crank-Nicolson finite difference scheme to obtain the solution. The detailed numerical method and procedure to solve the partial differential equation (1) is described below [29, 30].

The dependent variable C_p is a function of the independent variables x, z and t, i.e., $C_p = C_p(x, z, t)$. First, the continuum region of interest is overlaid with or subdivided into a set of equal rectangles of sides Δx and Δz, by equally spaced grid lines, parallel to z axis, defined by $x_i = (i-1)\Delta x,\ i = 1,2,3, \ldots$ and equally spaced grid lines parallel to x axis, defined by $z_j = (j-1)\Delta z,\ j = 1,2,3, \ldots$ respectively. Time is indexed such that $t_n = n\Delta t$, $n = 0, 1, 2, 3 \ldots$, where Δt is the time step. At the intersection of grid lines, i.e. grid points, the finite difference solution of the variable C_p is defined. The dependent variable $C_p(x, z, t)$ is denoted by, $C_{pij}^n = C_p\,(x_i, z_j, t_n)$, where (x_i, z_j) and t_n indicate the (x, z) value at a node point (i, j) and t value at time level n respectively.

We employ the implicit Crank-Nicolson scheme to discretize the equation (1). The derivatives are replaced by the arithmetic average of its finite difference approximations at the n^{th} and $(n+1)^{th}$ time steps. Then equation (1) at the grid points (i, j) and time step $n + 1/2$ can be written as

$$\left(\frac{\partial C_p}{\partial t}\right)_{ij}^{n+1} + \frac{1}{2}\left[U(z)\frac{\partial C_p}{\partial x}\Big|_{ij}^{n} + U(z)\frac{\partial C_p}{\partial x}\Big|_{ij}^{n+1}\right] + \frac{1}{2}\left[W(z)\frac{\partial C_p}{\partial z}\Big|_{ij}^{n} + W(z)\frac{\partial C_p}{\partial z}\Big|_{ij}^{n+1}\right] =$$

$$\frac{1}{2}\left[\frac{\partial}{\partial z}\left(K_z(z)\frac{\partial C_p}{\partial z}\right)\Big|_{ij}^{n} + \frac{\partial}{\partial z}\left(K_z(z)\frac{\partial C_p}{\partial z}\right)\Big|_{ij}^{n+1}\right] - \frac{1}{2}(k_{wp})(C_{pij}^{n} + C_{pij}^{n+1}) for\ i = 1,2,\ldots\ \ j = 1,2,\ldots \quad (34)$$

We use $\left.\frac{\partial C_p}{\partial t}\right|_{ij}^{n+\frac{1}{2}} = \frac{C_{pij}^{n+1} - C_{pij}^{n}}{\Delta t}$ (35)

This analog is actually the same as the first order correct analog used for the forward difference equation, but is now second order-correct, since it is used to approximate the derivative at the point$(x_i,\ z_j,\ t_{n+1/2})$. We use the backward differences for advective term for this model. Therefore we use $U(x,z)\frac{\partial C_p}{\partial x}\Big|_{ij}^{n} = U_{ij}\left[\frac{C_{pij}^{n} - C_{pi-1j}^{n}}{\Delta x}\right]$ (36)

$$U(x,z)\frac{\partial C_p}{\partial x}\Big|_{ij}^{n+1} = U_{ij}\left[\frac{C_{pij}^{n+1} - C_{pi-1j}^{n+1}}{\Delta x}\right] \quad (37)$$

$$W(z)\frac{\partial C_p}{\partial z}\Big|_{ij}^{n} = W_j\left[\frac{C_{pij}^{n} - C_{pij-1}^{n}}{\Delta z}\right] \quad (38)$$

$$W(z)\frac{\partial C_p}{\partial z}\Big|_{ij}^{n+1} = W_j\left[\frac{C_{pij}^{n+1} - C_{pij-1}^{n+1}}{\Delta z}\right] \quad (39)$$

Also, for the diffusion term, we use the second order central difference scheme

$$\frac{\partial}{\partial z}\left(K_z(z)\frac{\partial C_p}{\partial z}\right)\Big|_{ij}^{n} = \frac{K_z(z)\frac{\partial C_p}{\partial z}\Big|_{ij+1/2}^{n} - K_z(z)\frac{\partial C_p}{\partial z}\Big|_{ij-1/2}^{n}}{\Delta z} = \frac{1}{\Delta z}\left(\frac{K_{j+1}+K_j}{2}\right)\left(\frac{C_{pij+1}^{n} - C_{pij}^{n}}{\Delta z}\right) -$$

$$\frac{1}{\Delta z}\left(\frac{K_j + K_{j-1}}{2}\right)\left(\frac{C_{pij}^{n} - C_{pij-1}^{n}}{\Delta z}\right)$$

Hence,

$$\frac{\partial}{\partial z}\left(K_z(z)\frac{\partial C_p}{\partial z}\right)\Big|_{ij}^{n} = \frac{1}{2(\Delta z)^2}\left[(K_{j+1} + K_j)(C_{pij+1}^{n} - C_{pij}^{n}) - (K_j + K_{j-1})(C_{pij}^{n} - C_{pij-1}^{n})\right] \quad (40)$$

Similarly,

$$\frac{\partial}{\partial z}\left(K_z(z)\frac{\partial C_p}{\partial z}\right)\Big|_{ij}^{n+1} = \frac{1}{2(\Delta z)^2}\left[(K_{j+1} + K_j)(C_{pij+1}^{n+1} - C_{pij}^{n+1}) - (K_j + K_{j-1})(C_{pij}^{n+1} - C_{pij-1}^{n+1})\right] \quad (41)$$

Substituting equations (36) to (41) in equation (34) and rearranging the terms we get the finite difference equations for the primary pollutant C_p in the form

$$A_j C_{pi-1j}^{n+1} + B_j C_{pij-1}^{n+1} + D_j C_{pij}^{n+1} + E_j C_{pij+1}^{n+1} = F_j C_{pi-1j}^{n} + G_j C_{pij-1}^{n} + M_j C_{pij}^{n} + N_j C_{pij+1}^{n} \quad (42)$$

for each $i = 2,3,4, \ldots imaxl \ldots imaxX_0$, for each $j = 2,3,4, \ldots jmax - 1$ and $n = 0,1,2,3, \ldots$

where, $A_j = -U_j \frac{\Delta t}{2\Delta x}$, $F_j = U_j \frac{\Delta t}{2\Delta x}$, $B_j = -\left[\frac{\Delta t}{4(\Delta z)^2}\left(K_j + K_{j-1}\right) + W_j \frac{\Delta t}{2\Delta z}\right]$

$G_j = \left[\frac{\Delta t}{4(\Delta z)^2}\left(K_j + K_{j-1}\right) + W_j \frac{\Delta t}{2\Delta z}\right]$, $E_j = -\frac{\Delta t}{4(\Delta z)^2}\left(K_j + K_{j+1}\right)$, $N_j = \frac{\Delta t}{4(\Delta z)^2}\left(K_j + K_{j+1}\right)$

$D_j = 1 + U_j \frac{\Delta t}{2\Delta x} + W_j \frac{\Delta t}{2\Delta z} + \frac{\Delta t}{4(\Delta z)^2}\left(K_{j+1} + 2K_j + K_{j-1}\right) + \frac{\Delta t}{2}\left(k_{wp}\right)$

$M_j = 1 - U_j \frac{\Delta t}{2\Delta x} - W_j \frac{\Delta t}{2\Delta z} - \frac{\Delta t}{4(\Delta z)^2}\left(K_{j+1} + 2K_j + K_{j-1}\right) - \frac{\Delta t}{2}\left(k_{wp}\right)$

$i\,maxl$ and $imaxX_0$ are the i values at $x = l$ and X_0 respectively and $jmax$ is the value of j at $z = H$.

Equation (42) is true for interior grid points. At the boundary grid points we have to use the boundary conditions (2) to (5). The initial and boundary conditions can be written as $C_{pij}^0 = 0 \;\; for\; j = 1,2, \ldots j_{max},\; i = 1,2, \ldots imaxl \ldots imaxX_0$

$C_{pij}^{n+1} = 0 \;\; for \;\; i = 1 \; and \; j = 1,2, \ldots jmax \,,\; n = 0,1,2, \ldots$ (43)

$\left(1 + \left(w_s + V_{dp}\right)\frac{\Delta z}{K_j}\right) C_{pij}^{n+1} - C_{pij+1}^{n+1} = -\frac{Q\Delta z}{K_j}$ for $j = 1,\; i = 2,3,4, \ldots . imaxl$ and $n = 0,1,2,3 \ldots$ (44)

$C_{pijmax-1}^{n+1} - C_{pijmax}^{n+1} = 0 \;\; for \;\; j = jmax,\; i = 2,3,4, \ldots imaxl \ldots imaxX_0$ (45)

The above sets of equations are tridiagonal system and they are solved by using Thomas algorithm [31]. The ambient air concentration of primary pollutants (gaseous) is obtained for various atmospheric conditions and values of dry deposition and wet deposition.

5. Results and Discussion

The pollutants are assumed to be emitted at a constant rate from a uniformly distributed area source over a busy urban region up to $l = 6$ km downwind from the origin. We have computed the concentration of pollutants in the urban region with appropriate boundary conditions which take into account the impact of ground level area source and several removal mechanisms. We have taken the primary source strength $Q = 1\ \mu gm^{-2}s^{-1}$ at ground level from an area source and the mixing height is selected as 624 meters.

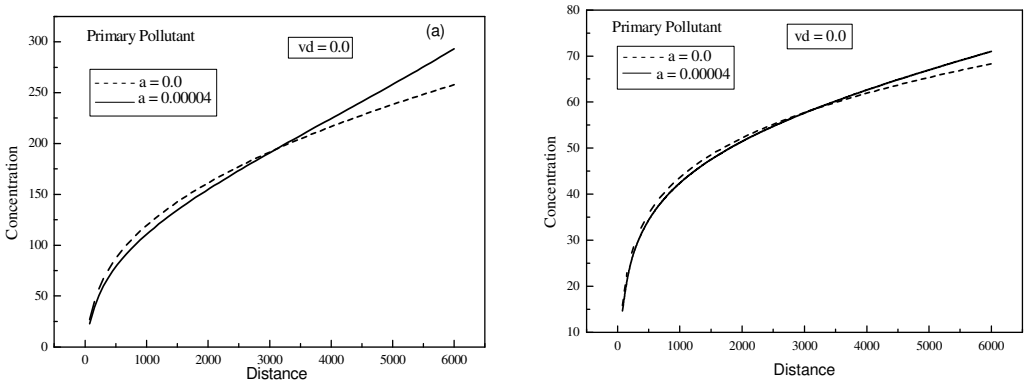

Fig 2: Variation of ground level concentration with respect to distance of primary pollutant for (a) Stable (b) Neutral case

In Figure 2 the effect of mesoscale wind on primary pollutant for the stable and the neutral cases is studied. The concentration of primary pollutants is less on upwind side of centre of heat island and more on downwind side of centre of heat island in the presence of mesoscale wind (a = 0.00004) compared to that in the absence of (a = 0) mesoscale wind. This is because the horizontal component of the mesoscale wind is along the large scale wind on the left and against it on the right. Thus, in the presence of mesoscale wind the advection is more on the left and less on the right. Therefore the concentration is less on the left and more on the right in the presence of mesoscale wind. In general the concentration of primary pollutant increases in the downwind direction.

In Figure 3 the concentration versus height of primary pollutant for the stable and the neutral cases is studied. The concentration of primary pollutants decreases as the height increases for the stable and the neutral cases. The primary pollutant is nearly zero at 25 meters height in the stable case and is nearly zero at 100 meters height in the neutral case. This shows that the neutral case enhances vertical mixing and the stable case suppresses vertical mixing. Therefore the ground level concentration is more concentrated in the stable case and is less concentrated in the neutral case.

In Figure 4 the effect of gravitational settling velocity and mesoscale wind on to primary pollutant for the stable and the neutral cases is studied. As gravitational settling velocity increases, the concentration of primary pollutant decreases. The concentration of primary pollutants decreases rapidly in the stable case and decreases slowly in the neutral case because the pollutants concentration is high in the stable case and low in the neutral case.

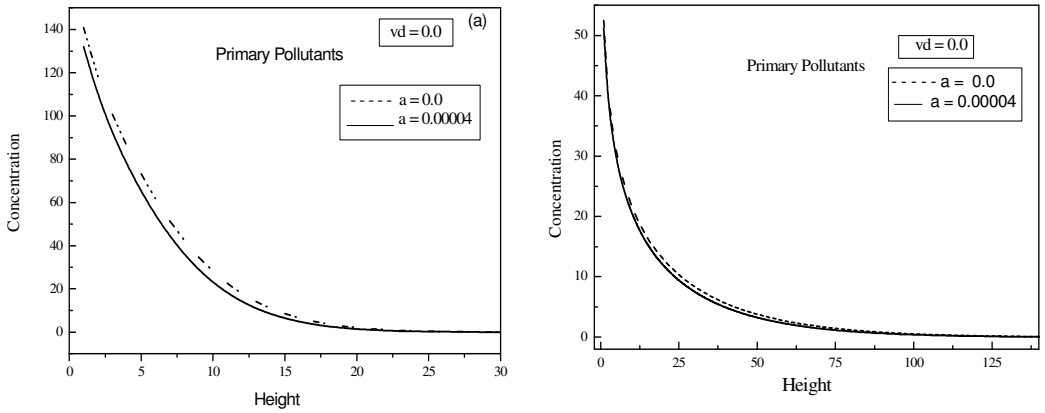

Fig 3: Variation of ground level concentration with respect to height of primary pollutant for (a) Stable (b) Neutral case

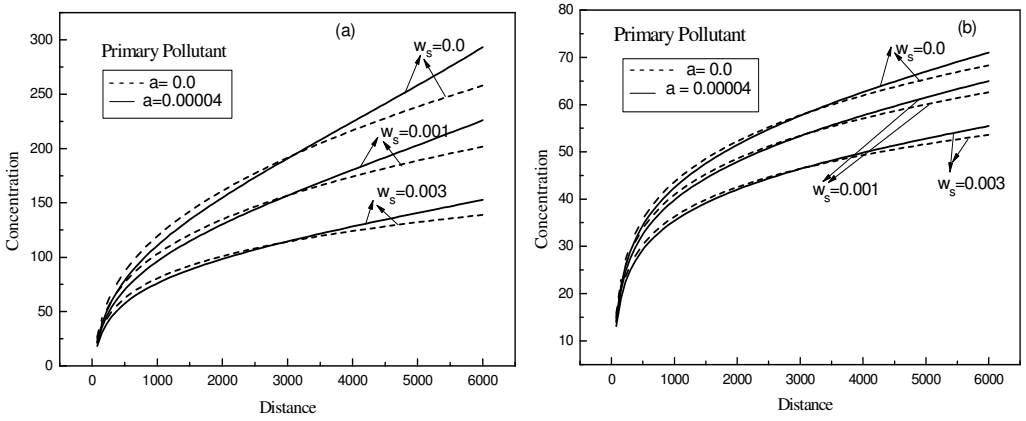

Fig. 4: Variation of ground level concentration with respect to distance of primary pollutant with various values of gravitational settling for (a) Stable (b) Neutral case

In Figure 5 the concentration versus height for primary pollutant for the stable and the neutral atmospheric cases are studied. The concentration of primary pollutant decreases as heights increases for the stable and the neutral cases. The primary pollutant is nearly zero at 25 metres height in the stable case and nearly zero at 100 meters height in the neutral case. This shows that the neutral case enhances vertical mixing and the stable case suppresses vertical mixing. Therefore the ground level concentration is more concentrated in the stable case and is less concentrated in the neutral cases for with and without mesoscale winds.

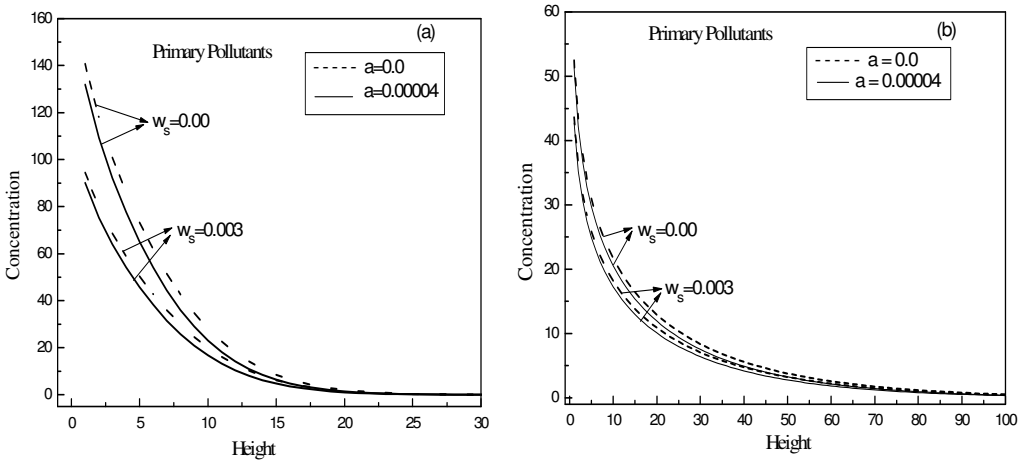

Fig. 5 Variation of ground level concentration with respect to height of primary pollutant with various values of gravitational settling for (a) Stable (b) Neutral case

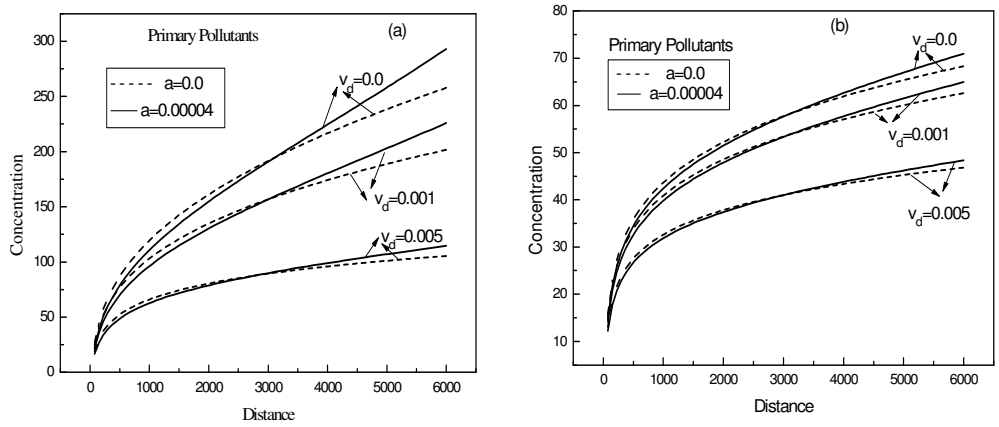

Fig. 6 Variation of ground level concentration with respect to distance of primary pollutant with various values of dry deposition for (a) Stable (b) Neutral case.

In Figure 6 the effect of dry deposition velocity with mesoscale wind (a-0.00004) and without mesoscale wind (a = 0) to primary pollutant for the stable and the neutral cases is studied. As dry deposition velocity increases the concentration of pollutants decreases. The concentration of primary pollutant decreases rapidly in the stable case and decreases slowly in the neutral case because the pollutants concentration is high in the stable case and low in the neutral case. In the presence of mesoscale wind (a = 0.00004) the concentration is less when compared to that in the absence of mesoscale wind (a = 0). The concentration of primary pollutant is less on the upwind sides of centre of that heat island (x = 3 km) and more on the downwind sides of centre of heat island in the presence of mesoscale wind (a = 0.00004) compared to that in the absence of mesoscale wind (a = 0). This is due to the

horizental component of mesoscale wind which is along the large scale wind on the left and against on the right.

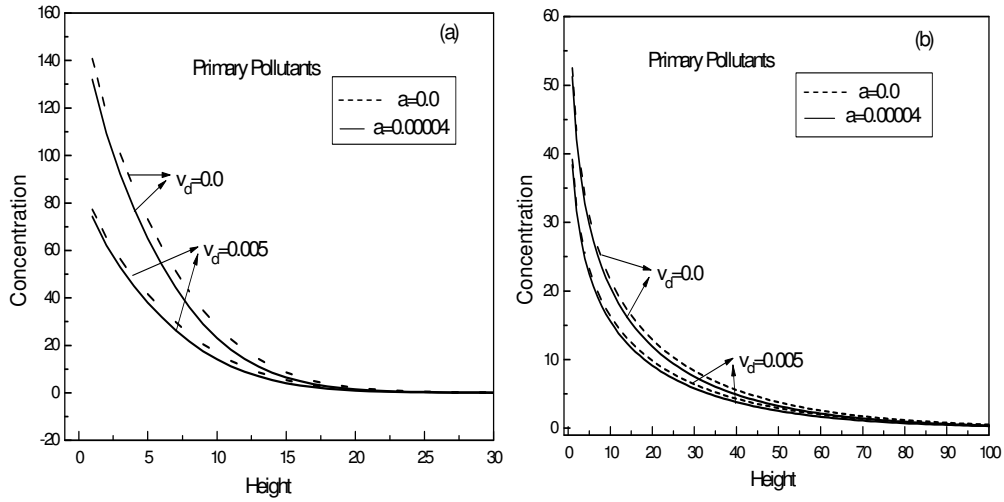

Fig. 7 Variation of ground level concentration with respect to height of primary pollutant with various values of dry deposition for (a) Stable (b) Neutral case

In Figure 7 the concentration of primary pollutant verses height for different dry deposition velocities with mesoscale wind (a = 0.00004) and without mesoscale wind (a = 0) for the stable and the neutral case is studied. As dry deposition velocity increases the concentration of primary pollutant decreases. The primary pollutant is nearly zero at 20 meters height in the stable case and is nearly zero at 90 meters height in the neutral case. The magnitude of pollutants concentration is higher in the stable case and is lower in the neutral case. This is because the neutral case enhances vertical diffusion to the greater heights and thus the concentration is less.

In Figure 8 the effect of wet deposition velocity with mesoscale wind (a-0.00004) and without mesoscale wind (a = 0) to primary pollutant for the stable and the neutral cases is studied. As wet deposition velocity increases the concentration of pollutants decreases. The concentration of primary pollutants decreases rapidly in the stable case and decreases slowly in the neutral case because the pollutants concentration is high in the stable case and low in the neutral case. In the presence of mesoscale wind (a = 0.00004) the concentration is less when compared to that in the absence of mesoscale wind (a = 0). The concentration of primary pollutant is less on the upwind sides of centre of that heat island (x = 3 km) and more on the downwind sides of centre of heat island in the presence of mesoscale wind (a = 0.00004) compared to that in the absence of mesoscale wind (a = 0). This is due to the

horizental component of mesoscale wind which is along the large scale wind on the left and against on the right.

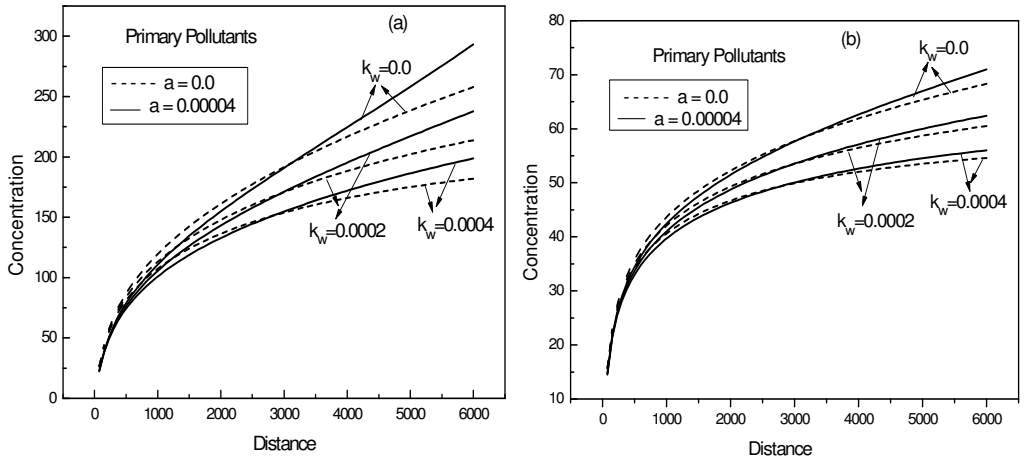

Fig. 8 Variation of ground level concentration with respect to distance of primary pollutant with various values of wet deposition for (a) Stable (b) Neutral case

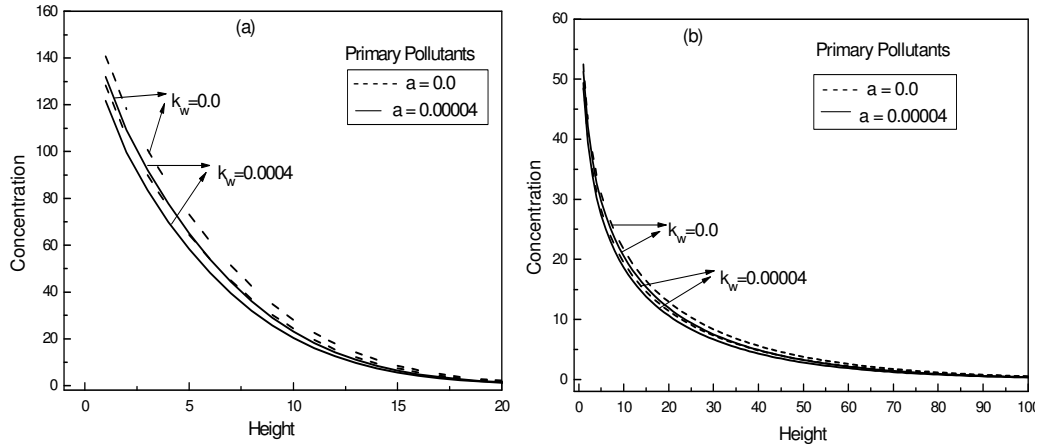

Fig. 9 Variation of ground level concentration with respect to height of primary pollutant with various values of wet deposition for (a) Stable (b) Neutral case

In Figure 9 the concentration of primary pollutant verses height for different wet deposition velocities with mesoscale wind (a = 0.00004) and without mesoscale wind (a = 0) for the stable and the neutral case is studied. As wet deposition velocity increases the concentration of primary pollutant decreases along the height. The primary pollutant is nearly zero at 17 meters height in the stable case and is nearly zero at 80 meters height in the neutral case. The magnitude of pollutants concentration is higher in the stable case and is lower in the neutral case. This is because the neutral case enhances vertical diffusion to the greater heights and thus the pollutant's concentration is less.

6. Conclusions

A two dimensional numerical model for air pollution in the presence of removal mechanisms and transformation process of the primary pollutant due to area source in an urban area for the stable and the neutral atmospheric situations with and without mesoscale wind is presented in this paper. This model takes into account the more realistic form of variable wind with mesoscale wind and eddy diffusivity profiles. This model analysis gives that the ground level concentration of primary pollutant attains peak value at the downwind end of the city. In the case of the stable atmospheric condition the concentration of primary pollutant is high at the surface region. But in the case of the neutral condition the pollutant concentration reaches more heights. This indicates that the neutral case enhances vertical diffusion of primary pollutant. Also the results obtained from the present work shows that mesoscale winds do not necessarily always reduce the pollution concentration but infect the opposite may occur depending on the location of the observer and the pollutant source, relative to the centre of the mesoscale wind and to the direction of large scale wind.

In order to clearly visualize the role of mesoscale wind (and hence of urban heat island) in shaping urban pollution pattern, the whole analysis has also been done in the absence of mesoscale wind and their comparative study shows substantial changes in pollution distribution. It has been found that the mesoscale wind aggravates the ground level concentration of air pollutants in the stable and the neutral atmospheric conditions. The results also demonstrate the increase in concentration level up to a considerable height under the mesoscale wind, thus it helps in circulating and moving the pollutants in vertical direction. It can be concluded that the presence of mesoscale wind enhances the concentration level of pollutants in urban areas for all vertical and downwind distances under all atmospheric conditions.

Though it is true, that now a day the air pollution situations are not handled in the way described in the present study. There are various air pollution situations that require the use of complex mesoscale models to adequately describe the processes and dynamics as well as incorporate chemistry and emissions in an adequate manner. Complex modeling studies such as CMAQ (Community Multiscale Air Quality Modeling) has been designed to approach air quality as a whole by including state of the science capabilities for modeling multiple air quality issues. However, in such complex models a number of processes viz. sea breeze circulations, urban heat islands, lee waves etc. going on inside them, so they appear as black boxes and one cannot easily understand the effects of individual processes on the air quality.

Apart from this, for many policy and scientific applications on air quality modeling, it is desirable not only to know the ambient pollutant concentration that would result from a certain situation, but also the extent to which those concentrations would change under various perturbations. Thus, the model proposed here helps in understanding one of these processes that is, urban heat island effect, by allowing control over environmental parameters. Hence, it would be easy to determine the steering factor for such a phenomenon and also to test its sensitivity against changes in atmospheric conditions. Thus, the results of the proposed model can be used to increase the credibility in complex model predictions and identify variables like wind field, atmospheric stability, etc. which should be investigated more closely in such complex modeling studies.

References

1. Pope I C A, Dockery D W, Schwartz J, Routlegde (1995) Review of Epidemiological Evidence of Health Effects of Particulate Air Pollution, Inhalation Toxicology 7: 1-18.

2**.** Brook R D, Franklin B, Cascio W, Hong Y, Howard G, Lipsett M, Luepker R, Mittleman: M, Samet J, Smith Jr S C, Tager I (2004) Air Pollution and Cardiovascular Disease: A Statement for Healthcare Professionals from the Expert Panel on Population and Prevention, Sci. Amer, Heart Assoc 109: 2655-2671.

3. Riediker M, Cascio W E, Griggs T R, Herbst M C, Bromberg P A, Neas L, Williams R.W., Devlin R B (2004) Particulate Matter Exposure in Cars Is Associated with Cardiovascular Effects in Healthy Young Men. Am. J. Respir. Crit. Care Med 169: 934-940. 10.1164/rccm.200310-1463 OC.

4. Arif A A, Shah S M (2007) Association between Personal Exposure to Volatile Organic Compounds and Asthma among US Adult Population. Int. Arch. Occup. Environ. Health 80: 711-719.

5. Oke T R (1995) Boundary Layer Climates. Inhalation Toxicology 7: 1-18.

6. Molders N, Olson M A (2004) Impact of Urban Effects on Precipitation in High Latitudes, Journal of Hydrometeorology 5: 409-429.

7. Haagensen P L, Morris AL (1974) Forecasting the behavior of the St. Louis, Missouri, Pollutant Plume.Journal of Applied Meteorology 13: 901-903.

8. Breeding R J, Haagensen PL, Anderson JA, Lodge Jr JP, Stampfer Jr JF (1975) The urban plume as see at 80 and 120 km by five different sensors, Journal of Applied Meteorology 14: 204- 216.

9. Ragland K W (1973) Multiple box model for dispersion of air pollutants from area sources. Atmospheric Environment 7: 1071-1089.

10. Runka E, Sardei F (1975) Numerical treatment of time dependent advection and diffusion of air Pollutants.Atmospheric Environment 9: 69-80.

11. Shir C C, Shieh L J (1974) A Generalized Urban Air Pollution Model and Its Application to the Study of SO_2 Distributions in the St. Louis Metropolitan Area, Journal of Applied Meteorology 13:185- 204.

12. Davidson B (1967) A Summary of the New York urban air pollution dynamics program, Journal of the Air Pollution Control Association 17: 154-158.

13. Chandler T J (1968) Discussion of the paper by MARSH and FPSTER The bearing of the urban temperature field upon urban pollution patterns, Atmospheric Environment 2: 619-620.

14. Dilley J F, Yen, K.T (1971) Effect of mesoscale type wind on the pollutant distribution from a line source.Atmospheric Environment Pergamon 5: 843-851.

15. Ermak D L (1977) An analytical model of air pollutant transport and dispersion from a point source. tmospheric Environment 11: 231-240.

16. Lee H N (1985) Three dimensional analytical models suitable for gaseous and particulate Pollutant transport, diffusion, transformation and removal, Atmospheric Environment 11:1951-1962.

17. Khan S K, M Venkatachalappa, Dulal Pal (1992) Three dimensional analytical model of Atmospheric dispersion of pollutant in a stable boundary line, International Journal of Environmental Studies, 41: 133-149.

18. Venkatachalappa M, Sujit Kumar Khan, Khaleel Ahmed G Kakamari (2003) Time dependent mathematical model of air pollution due to area source with variable wind velocity and eddy diffusivity and chemical reaction. Proceedings of the Indian National Science Academy 69, A, No.6: 745-758.

19. Khan S K (2000) Time dependent mathematical model of secondary air pollutant with instantaneous and delayed removal, Association for the Advancement of Modelling and Simulation Techniques in Enterprises 61: 1-14.

20. Rudraiah N, M Venkatachalappa, Sujit kumar Khan (1997) Atmospheric diffusion model of secondary pollutants. International Journal of Environmental Studies 52: 243-267.

21. Kakamari (2000) Mathematical modeling of air pollution Ph.D. thesis, Bangalore University.

22. Lakshminarayanachari K (2007) Mathematical modeling of air quality and dispersion, Ph.D. Thesis, Bangalore University.

23. Lakshminarayanachari K, Pandurangappa C, M Venkatachalappa (2011) Mathematical model of air pollutant emitted from a time defendant area source of primary and secondary pollutants with chemical reaction, International journal of computer applications in engineering, Technology and science 4: 136-142.

24. Monin A S, Obukhov A M (1954) Basic laws of turbulent mixing in the ground layer of the atmosphere. Doklady Akademii SSSR 151: 163-172.

25. Lettau H H (1970) Physical and Meteorological Basis for Mathematical Models of Urban Diffusion Processes, Proceedings of Symposium on Multiple Source Diffusion Models USEPA publication AP-86.

26. Shir C C (1973) A preliminary numerical study of a atmospheric turbulent flows in the idealized planetary boundary layer. Journal of Atmospheric Science 30: 1327-1341.

27. Ku J Y, Rao S T, Rao K S (1987) Numerical simulation of air pollution in urban areas model development, Atmospheric Environment 21(1): 201-214.

28. Jones P M, Larrinaga M A B, Wilson C B (1971) The urban wind velocity profile, Atmospheric Environment 5: 89-102.

29. Roache P J (1976) Computational fluid dynamics, Hermosa publications.

30. Wendt J F(1992) Computational fluid dynamics-An introduction (Editor), A Von Karman Institute Book, Springer-Verlag.

31. Akai T J (1994) Applied Numerical Methods for Engineers, John Wiley and Sons Inc: 6-90.